Molecular Biology of the Cell
Vol. 20, 438–451, January 1, 2009

LIM Kinase 1 and Cofilin Regulate Actin Filament Population Required for Dynamin-dependent Apical Carrier Fission from the *Trans*-Golgi Network

Susana B. Salvarezza,* Sylvie Deborde,* Ryan Schreiner,* Fabien Campagne,† Michael M. Kessels,‡ Britta Qualmann,‡ Alfredo Caceres,§ Geri Kreitzer,‖ and Enrique Rodriguez-Boulan*‖

*Margaret Dyson Vision Research Institute and ‖Department of Cell and Developmental Biology and †Department of Physiology and Biophysics, HRH Prince Alwaleed Bin Talal Bin Abdulaziz Alsaud Institute for Computational Biomedicine, Weill Medical College of Cornell University, New York, NY 10065; §Instituto de Investigacion Medica Mercedes y Martin Ferreyra, 5000 Cordoba, Argentina; and ‡Institute for Biochemistry I, Friedrich Schiller University Jena, 07743 Jena, Germany

Submitted September 2, 2008; Revised October 21, 2008; Accepted October 29, 2008
Monitoring Editor: Sandra L. Schmid

The functions of the actin cytoskeleton in post-Golgi trafficking are still poorly understood. Here, we report the role of LIM Kinase 1 (LIMK1) and its substrate cofilin in the trafficking of apical and basolateral proteins in Madin-Darby canine kidney cells. Our data indicate that LIMK1 and cofilin organize a specialized population of actin filaments at the Golgi complex that is selectively required for the emergence of an apical cargo route to the plasma membrane (PM). Quantitative pulse-chase live imaging experiments showed that overexpression of kinase-dead LIMK1 (LIMK1-KD), or of LIMK1 small interfering RNA, or of an activated cofilin mutant (cofilin S3A), selectively slowed down the exit from the *trans*-Golgi network (TGN) of the apical PM marker p75-green fluorescent protein (GFP) but did not interfere with the apical PM marker glycosyl phosphatidylinositol-YFP or the basolateral PM marker neural cell adhesion molecule-GFP. High-resolution live imaging experiments of carrier formation and release by the TGN and analysis of peri-Golgi actin dynamics using photoactivatable GFP suggest a scenario in which TGN-localized LIMK1-cofilin regulate a population of actin filaments required for dynamin-syndapin-cortactin–dependent generation and/or fission of precursors to p75 transporters.

INTRODUCTION

The organization of polarized intracellular trafficking to the plasma membrane (PM) involves a close cooperation between cargo proteins, adaptors and cytoskeletal elements that takes place at major sorting organelles, e.g., the Golgi complex and recycling endosomes (Bonifacino and Traub, 2003; Rodriguez-Boulan *et al*., 2005). Newly synthesized proteins destined for endosomes, lysosomes, and the basolateral PM of epithelial cells segregate into nascent post-Golgi or postendosomal vesicles via tyrosine, dileucine, or monoleucine sorting signals, clathrin adaptors, and accessory proteins (Bonifacino and Traub, 2003; Rodriguez-Boulan *et al*., 2005; Deborde *et al*., 2008).

By contrast, proteins destined for the apical PM are sorted into nascent post-Golgi transporters via *N*- and *O*-glycans, specialized transmembrane or cytoplasmic domains or glycosyl phosphatidylinositol (GPI)-anchors that interact with lipid domains (rafts), lectins, or microtubule (MT) motors (Scheiffele *et al*., 1995; Simons and Ikonen, 1997; Yeaman *et al*., 1997; Delacour *et al*., 2005, 2006; Rodriguez-Boulan *et al*., 2005). It is very well established that MT motors of the kinesin or dynein families play key roles in the generation and transcytoplasmic transport of tubular and vesicular transporters destined to the apical PM of Madin-Darby canine kidney (MDCK) cells (Kreitzer *et al*., 2000; Noda *et al*., 2001; Tai *et al*., 2001; Allan *et al*., 2002; Musch, 2004; Jaulin *et al*., 2007). By contrast, our knowledge of the specific roles of the actin cytoskeleton in intracellular transport routes remains fragmentary, unlike the situation at the PM, where various mechanisms involving the actin cytoskeleton in endocytic routes have been well documented (Erickson *et al*., 1996; Qualmann *et al*., 2000; Allan *et al*., 2002; Luna *et al*., 2002; Stamnes, 2002; Carreno *et al*., 2004; Matas *et al*., 2004; Bonazzi *et al*., 2005; Perret *et al*., 2005; Yarar *et al*., 2005; Egea *et al*., 2006; McNiven and Thompson, 2006).

The exit of cargo proteins from the *trans*-Golgi network (TGN) involves their concentration into vesicular or tubular transporters; various steps in the generation and fission of these transporters might involve the actin cytoskeleton and associated proteins. Studies in polarized epithelial cells (MDCK) have shown that the Rho GTPase cdc42, an actin cytoskeleton organizer found at the Golgi (Erickson *et al*., 1996; Kroschewski *et al*., 1999; Musch *et al*., 2001), actin-depolymerizing drugs (Lazaro-Dieguez *et al*., 2007), and Arp 2/3 (Rozelle *et al*., 2000; Guerriero *et al*., 2006) affect differentially the exit of apical and basolateral proteins from the TGN. In none of these cases, however, the specific roles of

This article was published online ahead of print in *MBC in Press* (http://www.molbiolcell.org/cgi/doi/10.1091/mbc.E08–08–0891) on November 5, 2008.

Address correspondence to: Enrique Rodriguez-Boulan (boulan@med.cornell.edu).

the actin cytoskeleton in cargo protein exit have been documented. The GTPase dynamin, which associates with the actin cytoskeleton to mediate fission of endocytic vesicles from the PM (Song *et al*., 2004), also mediates fission from the TGN of transport carriers for the apical protein p75 neurotrophin receptor (p75) in MDCK cells (Kreitzer *et al*., 2000; Bonazzi *et al*., 2005; Ya-Wen Liu *et al*., 2008). Interestingly, dynamin 2 mediates fission from the TGN of vesicular stomatitis virus G protein carriers in a cell-specific manner (Cao *et al*., 2000, 2005; Bonazzi *et al*., 2005). The cargo/cell-specific TGN fission activity of dynamin 2 may reflect cargo/cell specific requirements for its partners, cortactin and syndapin 2, involved in its recruitment to the TGN (Cao *et al*., 2005; Kessels *et al*., 2006; Yang *et al*., 2006). Additionally, these dynamin partners may contribute to the generation of post-Golgi routes through dynamin-independent functions, e.g., syndapin 2's abilities to promote actin filament assembly via Wiskott-Aldrich syndrome protein (WASP) or to bend membranes via its BAR domain (Kessels *et al*., 2006). The latter function of syndapin 2 could be critically needed, e.g., to shape tubular carriers, such as those used by apical cargo proteins to exit the TGN (Kreitzer *et al*., 2000, 2003).

Stow and coworkers (Percival *et al*., 2004) have shown that the Golgi complex displays a population of short and branched actin filaments. Practically nothing is known about the regulatory mechanisms involved in the organization of these Golgi filaments and about how these mechanisms contribute to the generation of specific cargo routes exiting the Golgi complex. A clue to actin filament organization at the Golgi may lie in recent studies on LIM kinases (LIMK) 1 and 2, widely expressed down-regulators of the actin-severing activity of cofilin that in neurons are known to operate downstream of cdc42 and PAK1(Bamburg, 1999; Foletta *et al*., 2004; Acevedo *et al*., 2006). Importantly, a study in hypocampal neurons (Rosso *et al*., 2004) showed that LIMK1 localizes to the Golgi complex via its LIM domains and to axonal growth cones via its postsynaptic density 95/disc-large/zona occludens domains and that overexpression of LIMK1 promotes axonal growth and differentiation. These experiments also showed that overexpression of wild-type LIMK1, or of various mutants of this protein, accelerated or slowed down axonal growth, promoted or inhibited accumulation of different axonal markers, and altered the dynamics of Golgi markers. Based on these results, Rosso *et al*. (2004) suggested that the changes in axonal morphogenesis they observed might result from regulation of Golgi protein trafficking by LIMK1. However, their experiments did not directly analyze the kinetics of cargo protein exit from the TGN and the long transfection times used (12 h) did not discard other equally likely interpretations of their data, i.e., that LIMK1 might alter the biosynthesis or degradation of axonal proteins, their cytoplasmic transport, or their delivery by vesicular fusion to the PM. Furthermore, although Rosso *et al*. (2004) showed that overexpression of LIMK1 or cofilin resulted in changes in actin levels at the Golgi, they neither carried out a detailed analysis of actin dynamics at the Golgi nor characterized the actin-based machinery required for cargo protein exit from the Golgi.

Here, we have rigorously tested the hypothesis that LIMK1-cofilin organizes a population of actin filaments at the Golgi complex that is required for polarized trafficking of cargo proteins out of this organelle. To this end, we characterized the roles of LIMK1-cofilin in endoplasmic reticulum (ER)-Golgi and post-Golgi trafficking of apical and basolateral cargo proteins in MDCK cells by using biochemical methods and quantitative live imaging protocols that we previously developed previously to measure the kinetics of Golgi exit of PM proteins (Kreitzer *et al*., 2000, 2003). In addition, we used MCDK cell lines expressing actin coupled to photoactivatable GFP (Patterson and Lippincott-Schwartz, 2002) to show that activated cofilin increased actin dynamics at the Golgi region. Other experiments demonstrated that these actin filaments were involved in recruiting dynamin 2 and suggest that the dynamin-interacting proteins cortactin and syndapin 2 are also involved in cargo protein exit from the Golgi complex. Together, our results conclusively show that LIMK1-cofilin organize a dynamic population of actin filaments at the Golgi region that shows remarkable selectivity in promoting the dynamin-mediated fission of carrier vesicles for the apical marker p75-green fluorescent protein (GFP) and a related receptor, NHR2, but not for a different apical marker, GPI-YFP, or for a basolateral marker, neural cell adhesion molecule (NCAM)-GFP. Our experiments constitute the first demonstration of a key trafficking role for LIMK1, cofilin, and actin filaments these proteins organize at the Golgi complex.

MATERIALS AND METHODS

Cell Culture

MDCK cells were cultured in DMEM (Invitrogen, Carlsbad, CA) containing 10% fetal bovine serum (FBS) at 37°C in 5% CO_2. Cells were seeded onto heat-sterilized, 25-mm round coverslips and grown for 48 h before microinjection. After injection, cells were maintained at 37°C in 5% CO_2 for 1 h 30 min allow the expression of injected cDNAs. Newly synthesized protein was accumulated in the TGN during a 30 min to 3h incubation at 20°C in bicarbonate-free DMEM with 5% FBS, HEPES, and 100 μg/ml cycloheximide (Sigma-Aldrich, St. Louis, MO). The synchronized release of p75-GFP, GPI-GFP, or NCAM-GFP after shifting to the temperature permissive for transport out of the Golgi (32°C) was monitored by time-lapse fluorescence microscopy in recording medium (Hanks' solution with 5% FBS, HEPES, glucose and 100 μg/ml cycloheximide) (Kreitzer *et al*., 2000). In other experiments, exit from Golgi was recorded in presence of and after a 10-min pretreatment with cytochalasin D (2 μM; Sigma-Aldrich) or jasplakinolide (100 nM; Calbiochem, San Diego, CA).

Microinjection

cDNAs were diluted in injection buffer (10 mM HEPES and 140 mM KCl, pH 7.4) before intranuclear microinjection by using back-loaded glass capillaries and a Narishige micromanipulator (Narishige, Tokyo, Japan). Cells were coinjected with cDNAs encoding p75-GFP (1 μg/ml), NCAM-GFP (10 μg/ml), or GPI-YFP (10 μg/ml) and LIMKs, cofilin, dynamin, syndapin 2, or cortactin mutants (20 μg/ml).

Live Imaging and Quantification of Fluorescence

Expression, accumulation in the TGN, time-lapse imaging and analysis of TGN exit rates for GFP-tagged markers in single cells, were performed as described previously (Kreitzer *et al*., 2000). p75-GFP and NCAM-GFP fluorescent images were collected using a Nikon inverted microscope (TE 300; Nikon, Tokyo, Japan) with fluorescein filter B-2E/C DM 505 (Chroma Technology, Brattleboro, VT) and a charge-coupled device camera (ORCAII-ER; Hamamatsu, Bridgewater, NJ). The acquisition and intensity measurements of the images were performed using MetaMorph imaging software (Molecular Devices, Sunnyvale, CA).

For quantitative measurements of cargo protein exit from TGN, cells were imaged using a 20× lens (Plan Fluor, numerical aperture [NA] 0.50), and images were collected at 15-min intervals for 5 h after the temperature shift (for p75-GFP), at 5-min intervals for 2.5 h (for NCAM-GFP), and at 10-min intervals for 3 h (for GPI-YFP). Expression of p75-GFP, NCAM-GFP or GPI-GFP always coincided with the expression of the LIMKs cofilin, dynamin, syndapin 2, or cortactin mutants when cDNAs were coinjected, as determined by immunofluorescence with anti-hemagglutinin (HA), FLAG, Xpress, or myc antibodies. For morphological analysis at the Golgi complex (high-magnification movies), cells were imaged one cell at a time by using a 100× lens (Plan Apochromat, NA 1.4), and images were collected at 1-s intervals for 1 to 2 min. To image p75-GFP containing post-Golgi carriers studies we coexpressed LIMK1-kinase-dead (KD) or cofilin S3A and p75-GFP, or dynamin 2 wild-type, LIMK1-KD, and p75-GFP. Live frames were acquired every 2 s for 3 min, by using a 40× objective to capture the entire cell. We have been successful in this type of triple microinjection experiments (Supplemental Figure 5). Expression of dynamin 2 and LIMK1-KD was assessed by immunofluorescence. p75-GFP–positive structures were scored as carriers provided they exhibited

the previously described vesicular or tubular shape and carrier velocity typical or kinesin transport (Kreitzer *et al*., 2000).

Quantification of p75-GFP at the Cell Surface

Transfection of the LIMK1-KD or cofilin S3A plasmid was performed by nucleofection with Amaxa technology by using 20 μg of cDNA/4 $\times$ 10^6 cells. Twenty-four hours later, subconfluent cells were injected with p75-GFP cDNA. Cells were incubated for 1h 30 min at 37°C to allow expression of p75-GFP, and then p75-GFP was accumulated in the Golgi by incubation at 20°C for 3 h. Cells were shifted to 32°C and fixed 0, 60, 120, and 240 min after release of the Golgi temperature block in 2% paraformaldehyde at room temperature for 2 min. p75-GFP at the cell surface was immunolabeled with a monoclonal antibody (mAb) that recognizes an extracellular epitope of p75, followed by Cy3-conjugated anti-mouse antibodies. Images of p75-GFP and anti-p75–injected cells were acquired using identical acquisition settings and exposure times for all samples in a single experiment. The integrated fluorescence intensities in GFP and anti-p75 images were measured, and the ratio anti-p75:p75-GFP intensities was calculated for each group of injected cells. The integrated fluorescence of 15–20 injected cells was measured at each time point. Finally, expression of LIMK1-KD and cofilin S3A were assessed by immunofluorescence after permeabilization with Triton X-100 during 7 min at room temperature.

Golgi Localization of Dynamin 2, Syndapin 2, and Cortactin

MDCK cells permanently expressing sialyl transferase fused to monomeric red fluorescent protein were transfected with LIMK1-KD alone or with LIMK1-KD + dynamin 2bb-GFP or syndapin 2-GFP constructs by nucleofection with Amaxa technology by using 20 μg of cDNA per 4 $\times$ 10^6 cells. Twenty-four hours after plating the cells at subconfluence, cells were fixed in 4% paraformaldehyde in 100 mM piperazine-*N*,*N*′-bis(2-ethanesulfonic acid), 5 mM EGTA, and 5 mM $MgCl_2$, pH 6.9, and stained with the dynamin mAb HUDY-1 or the cortactin polyclonal antibody (c-Tyr) and the antibody against HA-tag to visualized LIMK1-KD. The amount of dynamin, syndapin 2, and cortactin at the Golgi level under various experimental conditions was measured by digital microscopy (MetaMorph software) and expressed as the integrated dynamin or syndapin 2- or cortactin-specific fluorescence intensity at the TGN as a percentage of the total fluorescence in the cells.

Small Interfering RNA (siRNA)

To generate LIMK1 siRNA, we used oligonucleotides (nt) containing a 21 nucleotide sequence derived from canine LIMK1 transcript (GAACGUGGUGGUGGCUGACUU). As a negative control, we construct mutated LIMK1 siRNA in which two bases in the 21-nt target recognition sequence were mutated (GAACGUUGUGGUGGCUGCCUU). To silence LIMK 2, we used a 21-nucleotide sequence derived from canine LIMK2 (UGUUGACAGAGUACAUCGAUU). pSUPER construct targeted against luciferase was used as a negative control. The oligonucleotides were purchased from Dharmacon RNA Technologies (Chicago, IL). Transient transfection of the RNA interference (RNAi) plasmid was performed by nucleofection with Amaxa technology using 3 μg of oligonucleotides/4 $\times$ 10^6 cells. Cells were transfected a second time 72 h later and analyzed 48 h after the second transfection.

Measuring Actin Dynamics at the Golgi Region

MDCK cells permanently transfected with actin-photoactivatable (paGFP) were locally photoactivated at the Golgi region, identified by the exogenous Golgi-resident protein ST-mRFP, expressed by injection of its cDNA. For activation, we used a laser-scanning confocal microscope (model TCS SP2; Leica Microsystems, Deerfield, IL) with a 405-nm laser (20 mW) and a HCX PL APO 63×, 1.4 NA oil objective. Photoactivation was complete in ~1 s. The decay of fluorescence in the photoactivated region over time was monitored under 488-nm excitation at 0.8- to 1.6-s intervals for 3 min and used to measure the mobility of actin. At each time point after the transient Golgi localized activation, we also measured the fluorescence intensity at several regions of interest (ROIs), using LCS software (Leica Microsystems). Curves were generated from between 10 and 15 individual cells recorded for each experimental condition from two to three separate experiments. The photobleaching of GFP during the time of the experiment was negligible. To maximize the signal of paGFP, it was necessary to open the pinhole aperture to 2.75 airy. Noise reduction on fluorescence images was accomplished by subtraction of the fluorescence of an identically shaped region outside the cell. cDNAs encoding cofilin S3A and ST-mRFP were coinjected 4 h before the sequential time-lapse images were acquired. Jasplakinolide (100 nM) and latrunculin B (1 μM) were added to the recording medium ~10–20 min before the imaging. Differential interference contrast/Normarski images were collected to monitor changes in the cell shape due to the detachment from the coverslip induced by latrunculin B. Cells with excessive alterations in cell shape caused by the drug treatment were discarded.

The curves obtained from logarithmic transformation of the data (or from plotting the fluorescence data on semilogarithmic paper), were used to obtain the half-times of actin diffusion in the Golgi area. Actin diffusion coefficients were calculated from the equation $D = W^2/4\ t^{1/2}$, where W is the radius of the photoactivated Golgi region (6 μm in our experiments) and 4 $t^{1/2}$ is the half-time of diffusion (Kreis *et al*., 1982).

RESULTS

LIMK and Cofilin Selectively Regulate the Exit of p75-GFP from the TGN

To study the role of LIMK1, LIMK2, and cofilin in protein exit from the TGN, we comicroinjected nuclei of subconfluent MDCK cells with cDNAs encoding p75-GFP and the kinase-dead mutants LIMK1-KD or LIMK2-KD, which are known to behave as dominant-negative mutants (Arber *et al*., 1998; Sumi *et al*., 1999) or with cDNAs encoding constitutively activated cofilin (cofilin S3A). The cells were kept at 37°C for 1 h 30 min to allow synthesis of the proteins and at 20°C for an additional 3 h in the presence of cycloheximide, to allow exit of p75-GFP from the ER and accumulation in the TGN. Expression of LIMK and cofilin mutants did not interfere with the accumulation of p75-GFP at the Golgi complex (Figure 1A, top, 0 min) and did not noticeably alter Golgi morphology. Radioactive pulse-chase experiments confirmed that the transport of p75-GFP from ER-to-Golgi complex was not affected by LIMK1-KD (Supplemental Figure 1).

The second part of our pulse-chase imaging protocol was to change the cells to transport-permissive temperature, 32°C, to record the exit of p75-GFP by time-lapse microscopy, as described previously (Kreitzer *et al*., 2000). In control cells, p75-GFP underwent Golgi-to-plasma membrane transport within 4–5 h. After 315 min, p75-GFP was predominantly localized at the cell surface; correspondingly, fluorescence within the Golgi area was markedly reduced (Figure 1A, control, bottom, 315 min). By contrast, when we coinjected a plasmid encoding a kinase dead form of LIMK1, incapable of phosphorylating cofilin and down-regulating its activity (Rosso *et al*., 2004), the exit of p75-GFP from the Golgi area was strongly inhibited (Figure 1A, LIMK1-KD). Parallel experiments showed that LIMK1 but not LIMK1-KD promoted phosphorylation of cofilin at the Golgi region (data not shown). Expression of a constitutively active cofilin mutant also strongly inhibited the exit of p75-GFP (Figure 1A, cofilin S3A). Expression of kinase-dead LIMK2 also decreased Golgi exit, albeit to a much smaller extent than LIMK1-KD and Cofilin S3A (Figure 1A, LIMK2-KD).

Quantification of GFP fluorescence at the Golgi region (see *Materials and Methods*) at various short times (0–4 h) after transfer to transport-permissive temperature (Figure 1B) allowed us to directly measure the exit kinetics of p75-GFP from the Golgi complex under various experimental conditions. LIMK1-KD and Cofilin S3A drastically reduced the Golgi exit kinetics of p75-GFP; by contrast, LIMK2-KD only induced a moderate, albeit statistically significant, reduction of p75-GFP exit kinetics. We constructed a biochemical model of p75-GFP transport (see Supplemental Material) that included rate constants k_1 (p75-GFP export out from the endoplasmic reticulum to Golgi), k_2 (Golgi export of p75-GFP), and k_3 (degradation) (Figure 1C). This model illustrates that the total p75-GFP fluorescence stays constant in cells treated with LIMK1-KD (0.4% decrease after 200 min), whereas it decreases by 8, 6, and 5% after 200 min in control, cofilin S3A-, and LIMK2-KD-treated cells. This suggests that the decrease in total fluorescence in the latter three cases is probably due to a biological event, e.g., protein degradation after p75-GFP has reached the plasma membrane, and not to photobleaching, which would affect p75-GFP in a similar manner in any condition.

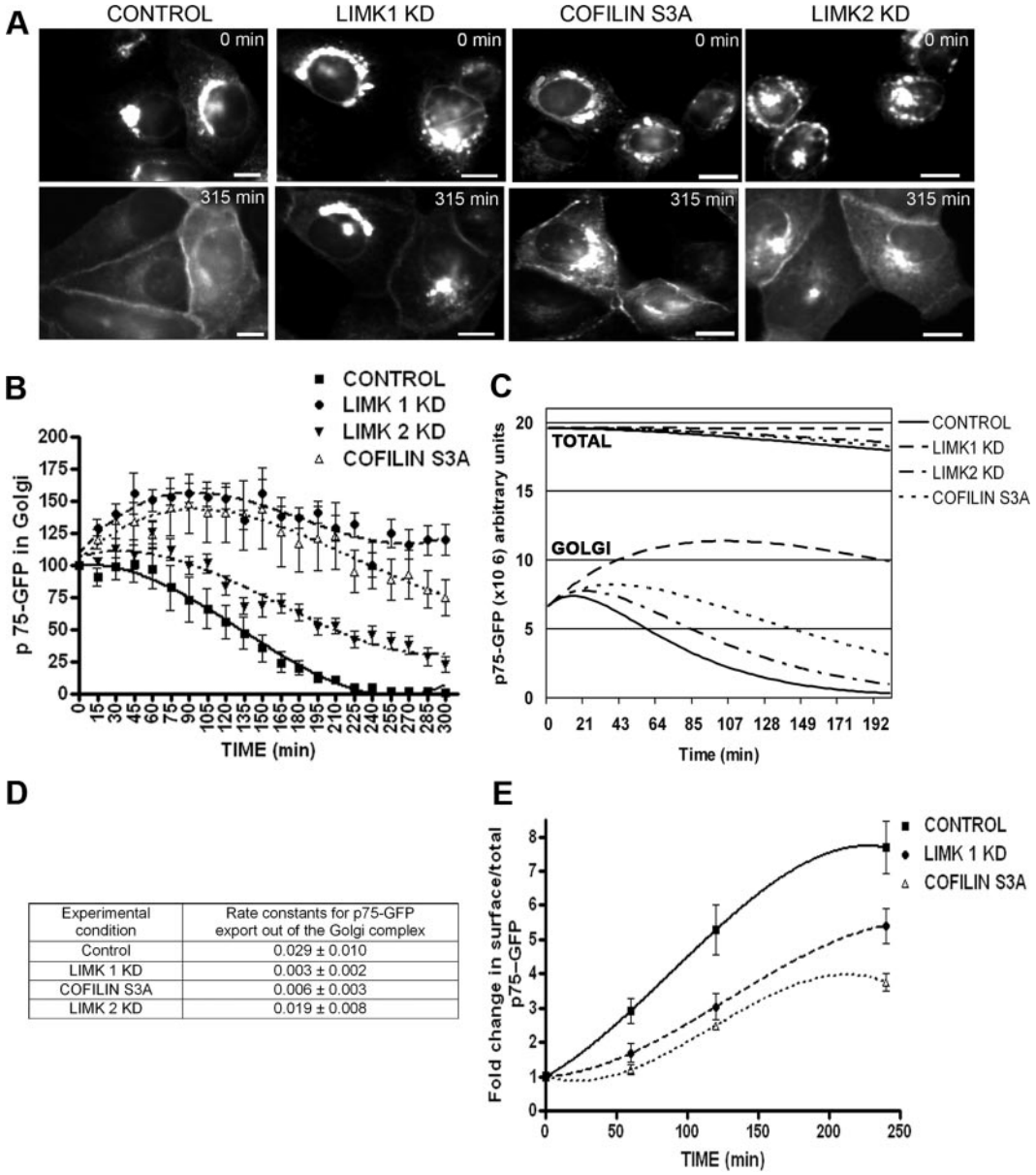

Experimental condition	Rate constants for p75-GFP export out of the Golgi complex
Control	0.029 ± 0.010
LIMK 1 KD	0.003 ± 0.002
COFILIN S3A	0.006 ± 0.003
LIMK 2 KD	0.019 ± 0.008

Figure 1. LIMK1-KD and cofilinS3A block Golgi exit and surface delivery of p75-GFP. (A) p75-GFP expressed by nuclear injection of its cDNA in subconfluent MDCK cells, accumulated in the TGN after a 20°C temperature block; its exit from TGN and transport to the plasma membrane were assessed after switch to transport-permissive temperature (32°C). Note surface arrival of p75-GFP after 315 min in control cells. By contrast, in cells coinjected with cDNAs encoding LIMK1-KD, cofilin S3A, or LIMK2-KD, p75-GFP was retained in the Golgi region. Bars, 20 μm. (B) p75-GFP fluorescence at the TGN was quantified for each condition after shift to 32°C (15–20 cells/experimental condition, experiments were repeated 2–3 times) and expressed as percent of TGN fluorescence at t = 0. Differences between control and LIMK or cofilin samples were statistically significant ($p < 0.0001$). (C) Fluorescence data were fitted to a mathematical model (see text). (D) Rate constants for TGN exit, obtained from this model, are expressed as mean ± SD. (E) Arrival of p75-GFP at the cell surface, measured as the ratio surface immunofluorescence/total GFP, was inhibited by LIMK1-KD and cofilin S3A expression ($p < 0.0001$).

Using this model, we calculated k_2 under the various experimental conditions (Figure 1D). For control cells, k_2 was 0.029 ± 0.010 min^{-1}. LIMK1-KD; cofilin S3A, and LIMK2-KD overexpression decreased k_2, respectively, to 0.003 ± 0.002 min^{-1} (9.6× reduction), 0.006 ± 0.003 min^{-1} (5× reduction) and 0.019 ± 0.006 min^{-1} (1.5× reduction).

In a separate group of experiments, we quantified the delivery of p75-GFP to the cell surface by measuring the ratio of surface-associated p75 (immunostaining with an ectodomain antibody) to total p75 (p75-GFP fluorescence intensity), as described previously (Kreitzer *et al.*, 2003). These experiments demonstrated a strong inhibition in p75-GFP surface transport caused by overexpression of LIMK1-KD or cofilin S3A (Figure 1E). Note that 250 min after release of the 20°C temperature block, 100% of p75-GFP has arrived at the plasma membrane in control cells, whereas in cells overexpressing LIMK1-KD, ~50% of the total p75-GFP has arrived at the cell surface, and the rest was retained at the Golgi complex (Figure 1, C and E). The apparently stronger inhibition of Golgi exit than of surface delivery of p75-GFP may be the result of the incoming p75-GFP from the ER that accumulates at the Golgi when

exit is inhibited by LIMK1 or cofilin S3A. Together, these experiments suggested an important role of LIM kinases in regulating the kinetics of p75-GFP exit from the TGN of MDCK cells.

LIMK1-KD and CofilinS3A Inhibit the Exit from the TGN of NHR2-GFP but Not of NCAM-GFP or GPI-Yellow Fluorescent Protein (YFP)

We next examined the effect of LIMK1-KD on exit from TGN of GPI-YFP, a lipid raft-anchored apical protein, of NCAM-GFP, a basolateral PM protein, and of NHR2-GFP, a PM protein structurally and functionally related to p75 (Murray *et al*., 2004). LIMK1-KD overexpression did not inhibit the exit of NCAM-GFP (Figure 2A) or GPI-YFP (Figure 2B) but strongly inhibited the exit from the TGN of NHR2-GFP (Figure 2C). Our results demonstrate that the regulatory roles of LIMK1 and cofilin on post-TGN trafficking are highly specific for a subset of PM proteins that currently only include p75-GFP and NHR2-GFP.

RNAi Suppression of LIMK1 but Not LIMK2 Inhibits p75-GFP Exit from the TGN

To test directly the involvement of LIMK1 and LIMK2 in the exit of p75-GFP from the TGN, we used an RNA interference (siRNA) approach. Introduction of LIMK1 or LIMK2 siRNAs that have been extensively characterized by other studies (Tomiyoshi *et al*., 2004, Chen and Macara, 2006) resulted in 72 and 95% reduction in the protein levels, respectively, as determined by immunoblot analysis 48 h after electroporation (Figure 3A). Efficient knockdown of LIMK1 and LIMK2 required two sequential electroporations, spaced 3 d apart. Knockdown of either LIMK1 or LIMK2 suppressed cofilin phosphorylation by ~74% without affecting the total levels of cofilin protein (Figure 3A). Strikingly, only LIMK1 knockdown induced a significant delay in the Golgi exit of p75-GFP (Figure 3B); LIMK2 knockdown had no effect (Figure 3C). The TGN exit rates of p75-GFP in MDCK cells treated with control siRNA (luciferase and mutated oligonucleotides) were faster than in microinjected parental MDCK cells. This may reflect different cellular responses to the different transfection protocols used in either case (microinjection in Figure 1 and electroporation in Figure 3).

LIMK1-KD inhibited the exit of p75-GFP from the TGN more drastically than LIMK1 siRNA (compare Figure 1B with Figure 3B). A possible explanation of this phenomenon is that whereas we could easily identify the population of cells expressing high levels of LIMK1-KD through the HA-tag added to LIMK1, it was difficult to identify a homogeneous population of cells expressing low levels of LIMK1 in siRNA experiments because appropriately sensitive antibodies were not available. Together, the results shown in Figure 1, 2, and 3 demonstrate that LIMK1 selectively regulates the exit of an apical route from the Golgi complex in MDCK cells.

LIMK1 but Not LIMK2 Localizes to the Golgi Apparatus

The different effects of LIMK1 and LIMK2 knockdown in post-Golgi transport were somewhat surprising considering the similarity of the two enzymes. To investigate whether the different trafficking regulatory activities of LIMK1-KD and LIMK2-KD on p75-GFP transport may be attributed to different subcellular localizations of LIMK1 and LIMK2, we studied the localization of endogenous and overexpressed LIMK1 and LIMK2 in MDCK cell lines expressing the *trans*-Golgi/TGN resident proteins Sialyltransferase-monomeric red fluorescent protein (Sialyl-T) (Figure 3D) or galactosyl transferase-cyan fluorescent protein (GalT) (Supplemental

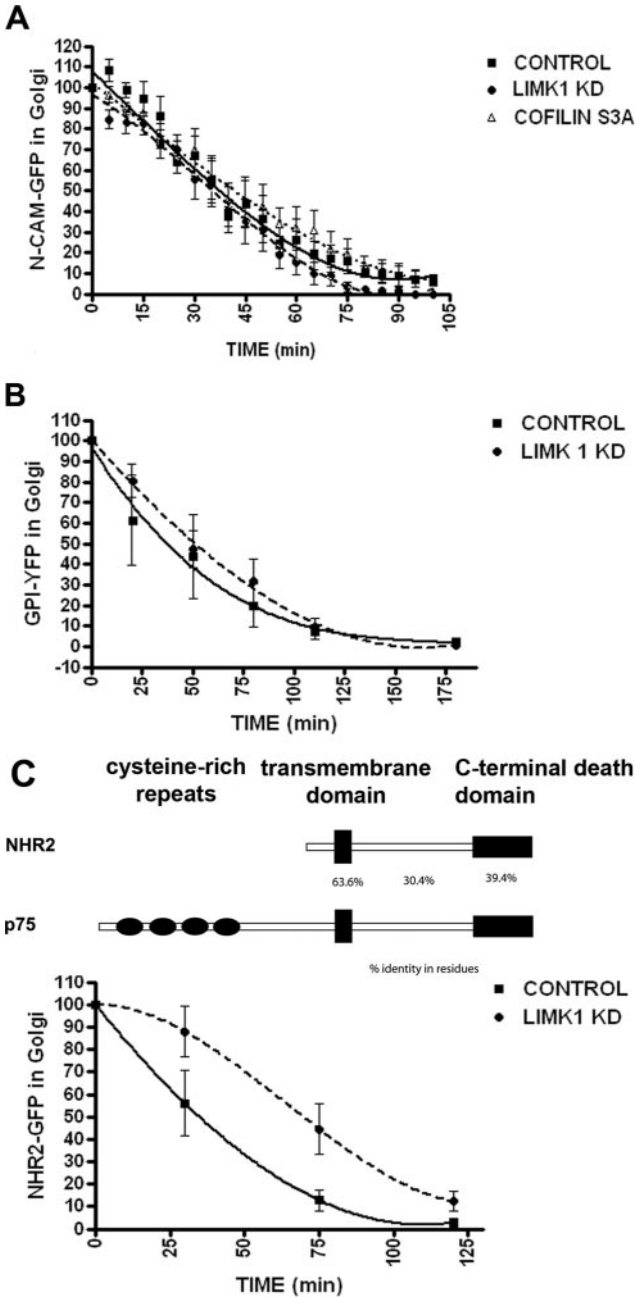

Figure 2. LIMK1-KD does not block exit from TGN of NCAM-GFP or GPI-YFP. The exit of NCAM-GFP (A), GPI-YFP (B), or NHR2-GFP, a protein related to p75 (C) from the TGN after shift to 32°C was recorded as described in *Materials and Methods* (2–3 experiments, 15–20 cells/experimental condition). Note that expression of LIMK1-KD does not interfere with the exit of NCAM-GFP or GPI-YFP from the TGN, but it does interfere with the exit of NHR2-GFP from the TGN. Expression of cofilin S3A does not affect the exit of NCAM-GFP.

Figure 2). Both endogenous LIMK1 (Figure 3D, top) and overexpressed LIMK1-KD (Supplemental Figure 2, top) colocalized extensively with Sialyl-T or Gal-T, in agreement with previous observations in neuronal cells (Rosso *et al*., 2004). Additional experiments showed that LIMK1 colocalized more precisely with TGN 38 (Figure 3E, left) than with the *cis*-medial Golgi marker Giantin (Figure 3E, right). Treatment of MDCK cells with nocodazole resulted in fragmen-

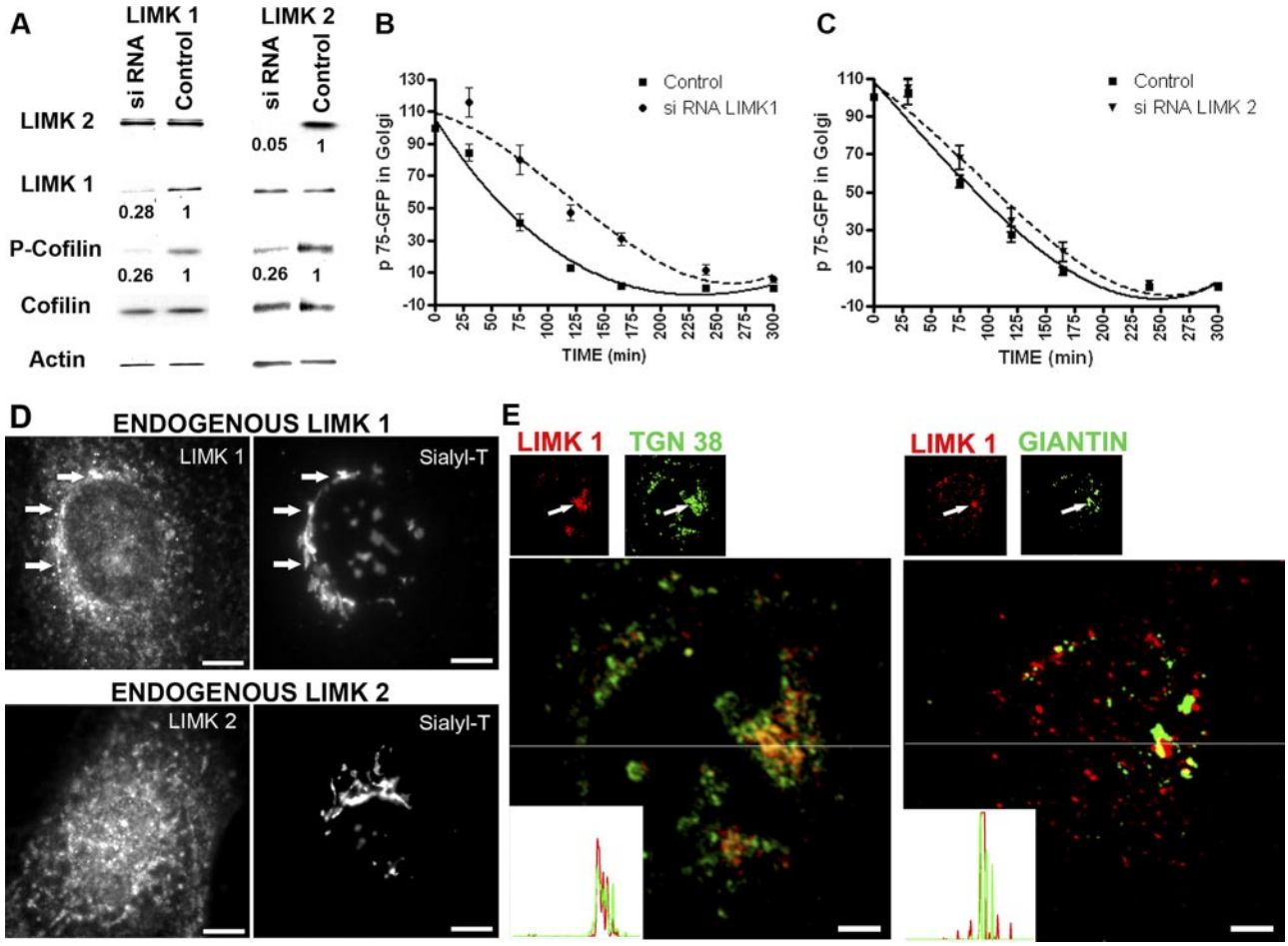

Figure 3. siRNA knockdown of Golgi-localized LIMK1 inhibits exit of p75-GFP from TGN. (A) MDCK cells were electroporated twice at 72-h intervals with control or canine LIMK1 and LIMK2 siRNA oligonucleotides, respectively, and analyzed 48 h later by immunoblot with antibodies for LIMK-1, LIMK-2, actin, Ser-3-phospho-cofilin, and cofilin. (B) The exit of p75-GFP from the TGN in these cells was recorded as in Figure 1B. LIMK1 siRNA inhibits the exit of p75-GFP from TGN ($p < 0.01$). (C) LIMK2 siRNA does not inhibit the exit of p75-GFP. (D and E) Subcellular localization of LIMK1 and LIMK2. (D) Endogenous LIMK 1 and 2: stable MDCK cell line expressing sialyltransferase-mRFP (sialyl-T) was labeled with anti-LIMK1 (top) or anti-LIMK 2 (bottom) antibodies. Note the colocalization of LIMK1 and Sialyl-T in the perinuclear region (top, arrows) and the absence of colocalization of endogenous LIMK 2 and Sialyl-T (bottom). Bars, 10 μm. (E) Colocalization of endogenous LIMK 1 with TGN 38 and Giantin: the spatial distribution of endogenous LIMK1 (red) and the Golgi resident proteins TGN 38 (*trans*-Golgi, left, green) and giantin (*cis*-medial Golgi, right, green) was determined using confocal imaging in sequential Z-axis planes made at every 240 nm. Two representative planes of one cell are shown. Note that LIMK1 colocalized more precisely with TGN 38 (left, arrows) than with the *cis*-medial Golgi marker Giantin (right, arrows). Insets show line profiles of the LIMK1 (red) and TGN 38 or giantin (green) fluorescence intensities from the lines in the magnified color combine views. Bars, 5 μm.

tation of the Golgi complex, with a concomitant dispersion of the LIMK1 staining, as expected for a Golgi-associated protein (data not shown). In contrast, both endogenous LIMK2 (Figure 3D, bottom) and overexpressed LIMK2-KD (Supplemental Figure 2, bottom) displayed a homogeneous distribution throughout the cytoplasm. These data strongly suggest that the more drastic inhibition of p75-GFP TGN exit by LIMK1-KD than by LIMK2-KD (Figure 1B) depends on the ability of the former to localize at the Golgi apparatus. We suggest that the small effect of overexpressed LIMK2-KD on p75-GFP trafficking can be attributed to inefficient competition with Golgi-localized LIMK1 for their substrate cofilin. By contrast, the lack of effect of LIMK2 siRNA on p75GFP exit from TGN (Figure 3C) can be attributed to the fact that LIMK2 siRNA should not have any effect on LIMK1 localization or function. Together, our data demonstrate that LIMK1-mediated activation of its downstream effector cofilin is strongly spatially restricted.

LIMK1-KD and Cofilin S3A Expression Inhibit Tubulation Dynamics of p75-GFP and Its Segregation from TGN Markers

To gain mechanistic understanding of the role of LIMK1 and cofilin in cargo exit from the TGN, we next analyzed by high-resolution live imaging the dynamic behavior of p75-GFP in the TGN after expression of LIMK1-KD or cofilin S3A. We showed previously that p75-GFP exits the TGN in tubules that rapidly extend and retract under the control of a kinesin motor and eventually undergo dynamin 2-dependent fission or/and vesiculation; both tubules and vesicles migrate on linear paths to the plasma membrane, where their fusion can be documented by total internal reflection fluorescence microscopy (Kreitzer *et al.*, 2000, 2003). Live imaging analysis in control cells demonstrated the presence of many dynamic tubules containing p75-GFP that extended and retracted from the Golgi complex at a rate of 0.25–1

μm/s with an average lifetime of 20 s; many of these tubules underwent vesicular fission from their tips (Figure 4A, left, and B). By contrast, cells expressing LIMK1-KD or cofilin S3A, displayed swollen and distended Golgi cisternae with long (10–15 μm) tubular processes displaying much longer lifetimes ($\geq$60 s) than those of control cells. These tubules did not retract back toward the Golgi (Figure 4A, right, and B) and did not generate vesicular carriers at their tips. Dual-color high-resolution imaging (1 frame s^{-1} for 1 min) of control cells expressing p75-GFP and ST-mRFP during the first 10 min after release from the 20°C block demonstrated that p75-GFP incorporated into tubules that were devoid of ST-mRFP (Figure 4C, left, arrows; see Supplemental Movie 1). In striking contrast, cells overexpressing LIMK1-KD or cofilin S3A displayed tubules containing either ST-mRFP alone (53 and 11%, respectively) or ST-mRFP plus p75-GFP (15–16%), with a dramatic reduction in the number of tubules containing only p75-GFP (Figure 4C, center and right panels; see Supplemental Movies 2 and 3 and quantification in Figure 4D). Many of these tubules displayed p75-GFP swellings (Figure 4C, asterisks).

Consistent with these observations, we observed a drastic decrease in the number of post-Golgi carriers for p75-GFP. When examined 10 min after release of the 20°C block, control cells exhibited numerous post-Golgi carriers for p75-GFP, identified as structures devoid of ST-mRFP moving toward the cell periphery with speeds of $\sim$0.5 μm/s, (Jaulin *et al*., 2007). By contrast cells treated with LIMK1-KD or cofilin S3A displayed a 90% reduction in the number of such carriers (Figure 4E and Supplemental Movies 4 and 5, quantification in right bar graph). The number of cytoplasmic carriers decreased in control cells 60 min after release of the 20°C temperature block, correlating with arrival of the protein to the cell surface, whereas they remained constant or slightly increased, respectively, in cells overexpressing LIMK1-KD or cofilin S3A (Figure 4E). Together, our results demonstrate that decreased LIMK function or increased cofilin activity lead to a dramatic decrease in the dynamics and fission of tubules that contain p75-GFP, resulting in a decrease in the number of post-Golgi carriers released into the cytoplasm.

Cooperation between LIMK1 and Dynamin 2 in Vesicle Fission from the TGN

Previous work by our laboratory (Kreitzer *et al*., 2000) and by others (Bonazzi *et al*., 2005) has shown that GTPase-deficient dynamin blocks exit of P75-GFP from the TGN by preventing fission of tubular transporters from the TGN, an effect strikingly similar to that observed in cells expressing LIMK1-KD and cofilin S3A (Figure 4). In contrast, it has been shown that recruitment of dynamin to the Golgi is dependent on actin and cortactin (Cao *et al*., 2005), as well as on syndapin 2 (Kessels *et al*., 2006). A unifying interpretation of these data are that the role of LIMK in the TGN is to promote the assembly of a population of actin filaments that are required for generation and dynamin-mediated fission of post-Golgi carriers for p75. A similar mechanism has been postulated for dynamin's regulation of endocytosis at the level of the plasma membrane (Qualmann *et al*., 2000; Conner and Schmid, 2003; Itoh *et al*., 2005), and actin might be required to provide the required tension in dynamin-dependent fission (Merrifield *et al*., 2005; Kaksonen *et al*., 2005). Such a scenario raised the possibility that LIMK1 might be acting upstream of dynamin 2 and that LIMK1-KD overexpression might therefore inhibit the stimulatory effect of dynamin on p75-GFP exit from the TGN.

Indeed, overexpression of wild-type dynamin 2 increased the number of post-Golgi carriers carrying p75-GFP relative to control cells (Figure 5A), as expected. Importantly, this stimulation was prevented by coexpression of LIMK1-KD (Figure 5A). The recruitment of dynamin 2 to the Golgi is partially dependent on its proline-rich domain (PRD). We found that overexpression of a truncated dynamin 2 that lacked the PRD (Dyn2 ΔPRD), or overexpression of dynamin's 2 PRD alone (Dyn2-PRD) (Cao *et al*., 2005) mimicked the inhibitory effect of LIMK1-KD on the exit of p75-GFP from the TGN albeit to a much smaller extent (Figures 1B and 5B). Quantitative analysis of fluorescent images showed that expression of LIMK1-KD decreased significantly the levels of endogenous dynamin 2 and overexpressed Dynamin 2bb-GFP at the Golgi (Figure 5C, left). The accompanying micrographs (Figure 5C, right) show an example of the higher recruitment of Dynamin 2 (bottom) at the Golgi complex (ST-mRFP; Figure 5C, middle) of control cells (asterisks, top) relative to LIMK 1 KD expressing cells. Together, our results are consistent with the possibility that LIMK1 and dynamin 2 cooperate in mediating fission of p75-GFP carriers from the TGN. Given that the effects of LIMK1-KD or actin depolymerization by cytochalasin D (see below) on Golgi exit are larger than the effects on dynamin 2 recruitment, the results suggest that actin plays a structural role in facilitating the function of dynamin, rather than a primary role in its recruitment. Furthermore, there may be overlapping mechanisms responsible for dynamin 2 recruitment.

As a next step, we focused on two actin regulatory proteins that bind the PRD of dynamin, syndapin 2 and cortactin. These proteins form Golgi complexes with dynamin 2 via their SH3 domains (Cao *et al*., 2005; Kessels *et al*., 2006) and may be expected to regulate Golgi trafficking via their interactions with the actin cytoskeleton in the vicinity of this organelle (Qualmann and Kelly, 2000, Cao *et al*., 2003; Kessels *et al*., 2006). Overexpression of LIMK1-KD decreased the levels of syndapin 2 and cortactin at the Golgi (Figure 5D). Furthermore, the overexpression of a truncated form of cortactin lacking 50 amino acids of the Src homology (SH)3 domain (CortΔSH3) or of the SH3 domain of syndapin (syndapin 2 SH3) strongly inhibited the Golgi exit of p75-GFP (Figure 5E). Interestingly, the truncated form of cortactin did not inhibit the Golgi exit of NCAM (Supplemental Figure 3). Together with the observed effects for Dyn2 ΔPRD and Dyn2-PRD described above, these experiments suggest that syndapin 2 and cortactin cooperate with dynamin 2 and LIMK1 to promote Golgi exit of p75-GFP. It is likely that, in addition to promoting dynamin 2 recruitment, syndapin 2 might independently facilitate p75 exit from TGN by promoting the formation of tubular carriers via its BAR domain. Additional work is necessary to understand the nature of the linkages between syndapin, cortactin, and dynamin that regulate Golgi trafficking.

TGN-trafficking Effects of LIMK1-KD and Cofilin S3A on p75-GFP Are Consistent with Increased Local Actin Filament Depolymerization

All conditions we found that inhibit p75-GFP exit from the TGN, i.e., overexpression of LIMK1-KD or cofilin S3A, as well as LIMK1 siRNA, are consistent with a local increase in cofilin activity. Cofilin severs actin filaments and generates new free barbed ends; it is generally believed that this leads to increased filament turnover (Carlier *et al*., 1997; Lappalainen and Drubin, 1997; Arber *et al*., 1998). However, during cell migration, local increases in cofilin activity may lead to actin filament formation (Ghosh *et al*., 2004). Hence, we used

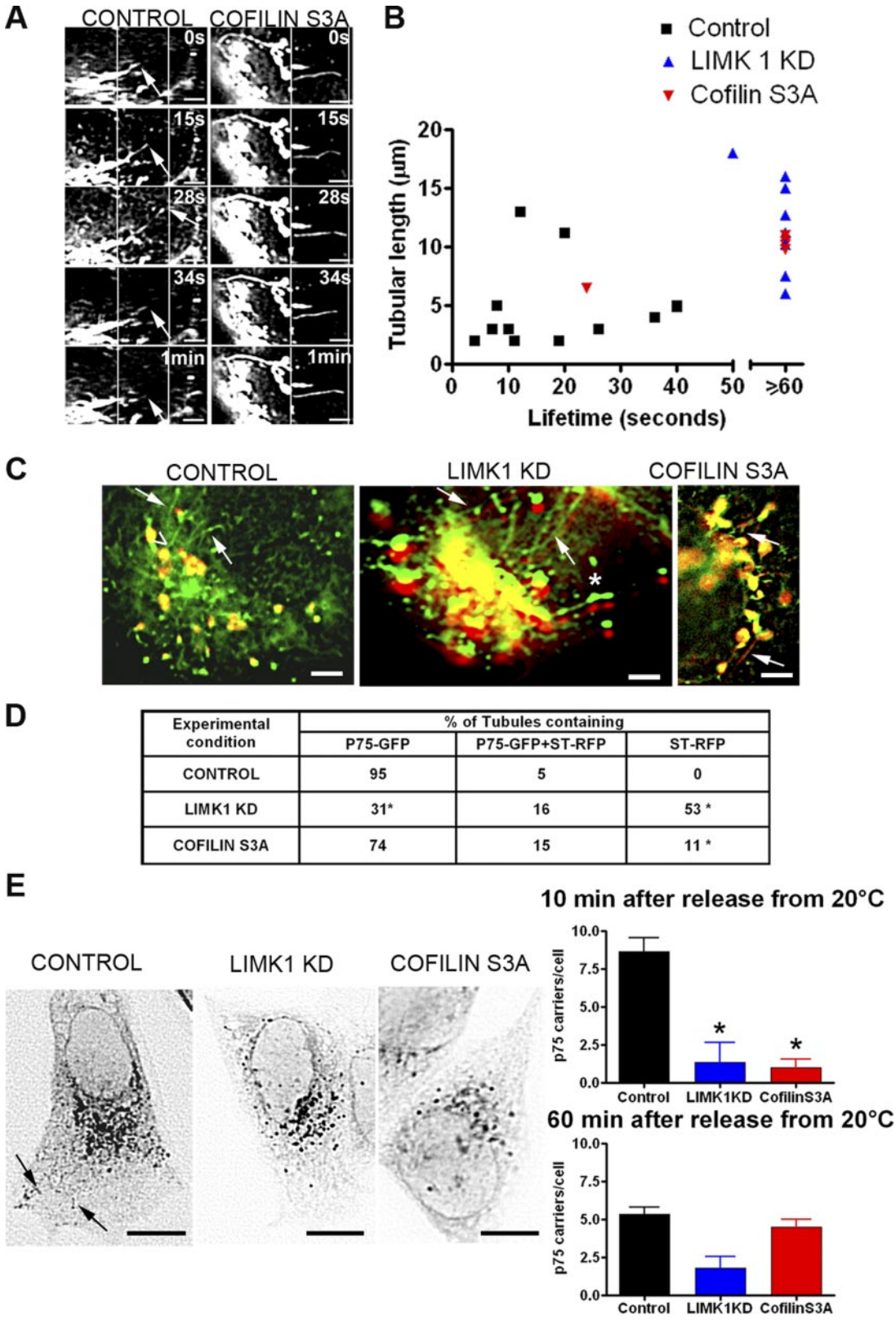

Experimental condition	% of Tubules containing		
	P75-GFP	P75-GFP+ST-RFP	ST-RFP
CONTROL	95	5	0
LIMK1 KD	31*	16	53 *
COFILIN S3A	74	15	11 *

Figure 4. LIMK1-KD and cofilinS3A disrupt the dynamics of tubulation of p75-GFP and its segregation from TGN markers. (A) A cDNA encoding p75-GFP was injected alone or together with a cDNA encoding for cofilin S3A into the nuclei of subconfluent MDCK cells. The formation of tubular precursors to post-Golgi transporters was analyzed 10 min after release of the 20°C block by high-resolution microscopy (time-lapse images acquired at ~1-s intervals for 1 min). Control cells (left) show extension and retraction of a p75-GFP tubule within <1 min (arrow on tubule tip). Cofilin S3A (right) induced long static tubules with no extension-retraction behavior. Bars, 5 μm. (B) Lengths and life-times of p75-GFP tubules in control, cofilin S3A or LIMK1-KD expressing cells. (C) Dual-color high-resolution images of cells expressing p75-GFP, LIMK1-KD, or Cofilin S3A and ST-mRFP were acquired as described in A. Control: note the exclusion of ST-mRFP from tubules

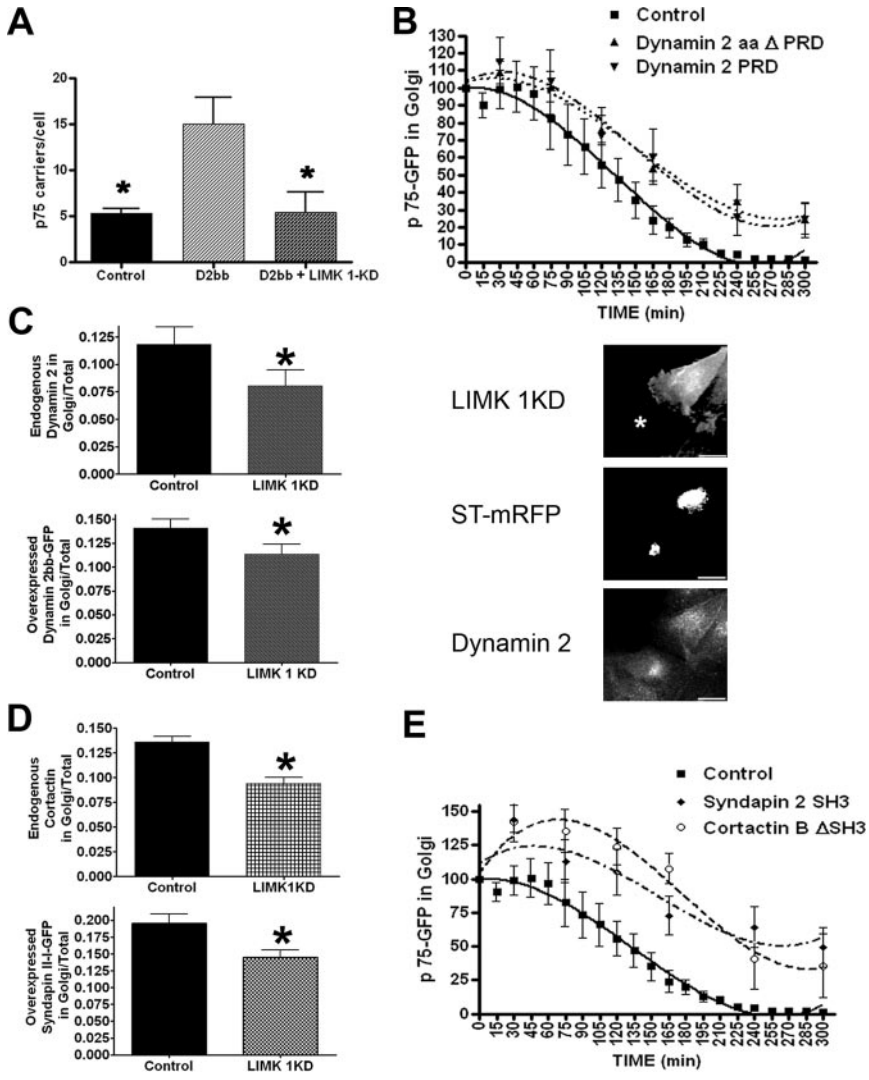

Figure 5. LIMK 1 activity induces recruitment of dynamin 2, which promotes fission of p75-GFP transporters likely assisted by cortactin and syndapin 2. (A) The release of post Golgi transporters was measured as in Figure 4E in cells expressing dynamin 2 ± LIMK1-KD, 120 min after release from 20°C block (6 cells/condition, 3 experiments). Asterisk indicates statistically significant differences ($p < 0.01$). (B) Overexpression of dynamin 2 proline-rich domain or dynamin 2 lacking its domain (Dynamin 2 ΔPRD) inhibited release of p75-GFP from the TGN ($p < 0.05$). (C) Recruitment of endogenous and overexpressed dynamin 2bb to the Golgi was inhibited by overexpression of LIMK1-KD (40 cells/condition, 2 experiments) ($p < 0.05$). Images (right) show an example of the higher recruitment of Dynamin 2 (bottom) at the Golgi (ST-mRFP, middle) of control cells (asterisks, top) compared with LIMK 1 KD-expressing cells. Bars, 20 μm. (D) Recruitment of endogenous cortactin and overexpressed syndapin 2 to the Golgi was inhibited by expression of LIMK1-KD (35 cells/condition, 2 experiments) ($p < 0.05$). (E) Overexpression of Syndapin 2 SH3 or cortactin ΔSH3 inhibited exit of p75-GFP from the TGN ($p < 0.05$).

two independent approaches to determine whether the trafficking effects caused by increased cofilin activity at the Golgi level might be mediated by increased actin filament polymerization or depolymerization.

Figure 4 (cont). containing p75-GFP (arrows, base marked by arrowhead). See also Supplemental Movie 1. Note that in cells expressing LIMK1-KD or cofilin S3A, emerging tubules (arrows) contain both p75-GFP (green) and ST-mRFP (red). The green and red images in LIMK1-KD were shifted by five pixels. See Supplemental Movies 2 and 3. Asterisk (*) marks swellings containing both proteins. Bars, 5 μm. (D) Quantification of tubules that contain p75-GFP, p75-GFP+ST-mRFP, or ST-mRFP alone under different experimental conditions (n = 10 cells/condition, 3 experiments). Asterisks (*) mark statistically significant differences compared with control. (E) Release of post-Golgi carriers (PGCs). MDCK cells expressing p75GFP were imaged (1- to 2-s intervals for 3 min) 10 min after release from 20°C. In control cells (left), P75-GFP is seen in the perinuclear region and in tubular and spherical PGCs accumulated within the cytoplasm (arrows). PGCs and their characteristic tracks can be seen in Supplemental Movie 4. On expression of LIMK 1-KD or cofilin S3A, the number of mobile p75 PGCs is drastically reduced, as seen in Supplemental Movie 5. Bar graphs: quantification of PGCs demonstrates a statistically significant difference ($p < 0.01$) between control and LIMK1-KD or Cofilin S3A injected-cells (6 cells/condition, 3 separate experiments).

As a first approach, we investigated whether the effect of LIMK1-KD and cofilin S3A mimicked the effect of stimulators or inhibitors of actin filament disassembly, e.g., cytochalasin D or jasplakinolide, respectively. Actin immunofluorescence and phalloidin staining demonstrated that expression of LIMK1-KD or cofilin S3A, like cytochalasin D, disrupted the delicate organization of actin filaments in the perinuclear region resulting in the accumulation of small actin aggregates; jasplakinolide, instead, induced the formation of large perinuclear actin aggregates, as previously described (Spector *et al*., 1999) (Figure 6 A and B, top; and Supplemental Figure 4C). Importantly, cytochalasin D (Figure 6A) but not jasplakinolide (Figure 6B) strongly inhibited the exit of p75-GFP from the TGN, confirming our previous report that latrunculin B delays the TGN exit of p75-GFP during the first 30 min after release of the 20°C transport block (Musch *et al*., 2001). For the experiments reported here, we used cytochalasin D because it did not promote cell detachment during the 5 h required to measure p75-GFP exit, unlike latrunculin B. Interestingly, cytochalasin D induced the formation of long TGN tubules labeled with ST-mRFP (Supplemental Figure 4B) similar to those we observed in cells overexpressing LIMK1-KD or cofilin S3A (Figure 4, A–C). These results are consistent with the hypothesis that the effects of LIMK1-KD and Cofilin S3A on

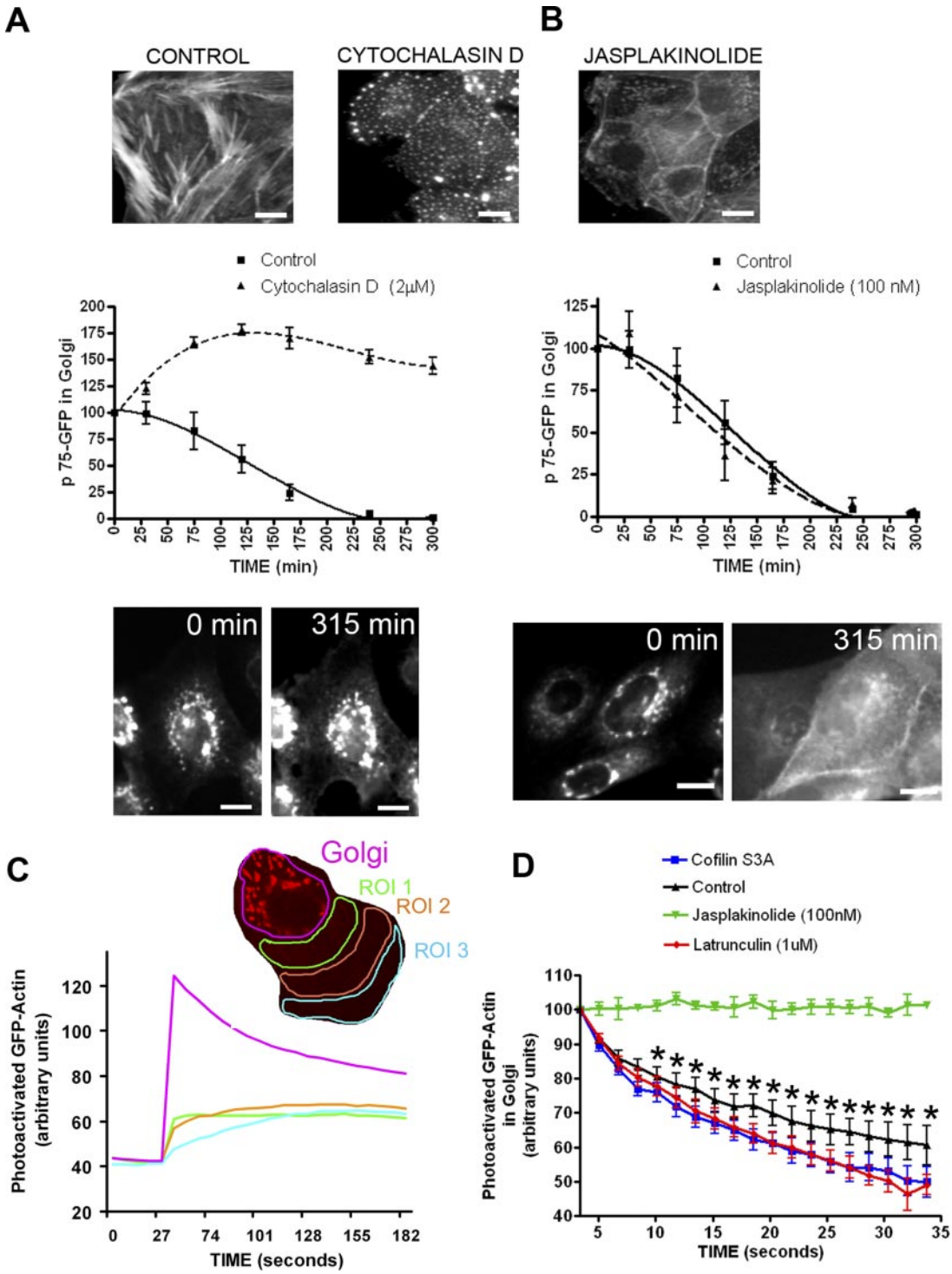

Figure 6. Exit of p75-GFP from TGN is blocked by increased actin filament depolymerization. (A and B) Phallodin staining of control, cytochalasin D (2 μM)-, and jasplakinolide (100 nM)-treated cells after a time-lapse record. Bars, 20 μm. Cytochalasin D (A) but not jasplakinolide (B) inhibits exit of P75-GFP from the TGN and prevents its redistribution to the plasma membrane ($p < 0.0001$; 10 cells in two separate experiments were quantified for each condition). Representative p75-GFP fluorescence images are shown at the bottom of each graph. Bars, 10 μm. (C and D) MDCK cell line expressing actin-paGFP was photoactivated at the Golgi region, defined by the presence of ST-mRFP (red). GFP fluorescence at the Golgi region and at more distant regions of interest in the cytoplasm (ROI 1–3) was subsequently recorded. Note in C that GFP fluorescence decays at the Golgi area but rises at other ROIs, indicating diffusion of actin monomers. (D) Curves represent decay of actin-paGFP fluorescence in Golgi area (5–12 cells/condition). Note biphasic decay in control cells. Fluorescence decay is blocked by jasplakinolide but is faster than in control cells upon Cofilin S3A or latrunculin B presence. Data are represented as mean ± SEM. Asterisks (*) indicate statistically significant differences ($p < 0.001$) between control and latrunculin B as well as between control and cofilin S3A effects.

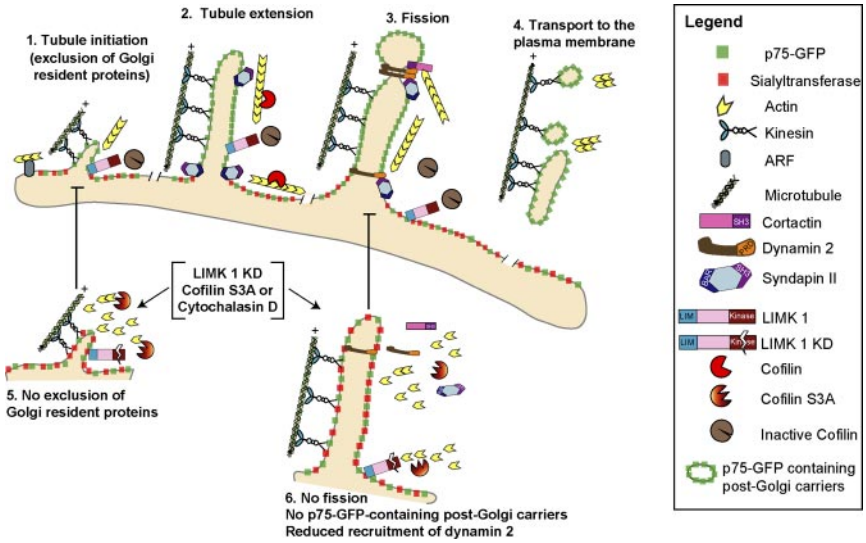

Figure 7. Model. LIMK1 and cofilin regulate a peri-TGN actin filament network required for the dynamin-dependent exit of p75-GFP. (1) A population of actin filaments, anchored to the TGN by an ARF-dependent mechanism (Percival *et al*., 2004; Cao *et al*., 2005) and regulated by cofilin and Golgi anchored LIMK1, which inactivates cofilin locally (Rosso *et al*., 2004; this study) facilitates the initial assembly of transporters for p75-GFP in cooperation with a plus-end–directed kinesin (Jaulin *et al*., 2007). Note that Golgi markers are excluded from these transporters. (2) p75GFP-containing tubules extend along MT drawn by a kinesin motor; syndapin 2, via its BAR-domain, binds to the membrane curvature of the Golgi (Kessels *et al*., 2006) and facilitates membrane remodeling necessary for tubulation. (3) p75-GFP tubules undergo fission from the TGN or into smaller transport vesicles; this process depends on actin filaments (regulated by LIMK 1-cofilin), which recruit cortactin, as well as syndapin 2. These two molecules recruit dynamin 2 via their SH3 domains and dynamin PRD (Cao *et al*., 2005; Kessels *et al*., 2006). (4) After dynamin-mediated fission, tubular and vesicular carriers for p75-GFP are transported by a plus-end kinesin along MT to the plasma membrane. (5) Inactivation of LIMK1 or overexpression of constitutively activated cofilin inhibits the segregation of p75 from TGN markers. (6) This treatment also inhibits dynamin-mediated fission of p75 transporters from TGN as well as the recruitment of Dynamin 2, syndapin 2, and cortactin to the Golgi.

post-Golgi trafficking of p75-GFP are mediated by increased actin filament disassembly.

As a second test of whether cofilin S3A promotes or inhibits actin filament disassembly at the Golgi, we measured local actin dynamics in the Golgi area under various experimental conditions. To this end, we generated an MDCK cell line that expresses actin linked to actin-paGFP (Patterson and Lippincott-Schwartz, 2002). Actin-paGFP incorporated into stress fibers and actin filaments at the level of the Golgi that were altered by treatment with actin-toxic drugs similarly as endogenous actin (Supplemental Figure 4C). We activated paGFP in the Golgi area defined by ST-mRFP, with laser illumination at 405 nm under examination by a confocal microscope and then measured the decay of GFP fluorescence as an indicator of actin dynamics in that region (see *Materials and Methods*) (Figure 6C). The decay of actin-GFP fluorescence in the Golgi area correlated with the progressive appearance of GFP fluorescence in regions of the cytoplasm away from the Golgi area, which is compatible with actin diffusion rather than with GFP photobleaching (Figure 6C). In control cells, this decay exhibited a fast component ($t_{1/2}$ = 22 s) and a slow component ($t_{1/2}$ = 54 s), which we presumed corresponded, respectively, to the diffusion of free actin monomer pool and actin filament turnover in the Golgi area (Figure 6D, black line) (McGrath *et al*., 1998). On treatment with jasplakinolide, the diffusion of actin-GFP was dramatically blocked (Figure 6D, green line). By contrast, treatment with latrunculin B (Figure 6D, red line) and with cofilin S3A (Figure 6D, blue line) significantly decreased the half-life of decay of the slow component compared with control cells ($t_{1/2}$ = 34 s and $t_{1/2}$ = 41 s, respectively; both $p < 0.001$). These results strongly suggest that increased cofilin activity promotes increased actin filament turnover at the Golgi level.

Thus, two independent experimental approaches are consistent with a scenario in which inhibition of LIMK1 activity at the Golgi region and the consequent activation of cofilin, the only established physiological substrate of LIMK1 (Arber *et al*., 1998, Bernard, 2007), increases local actin filament disassembly, which in turn delays the exit of p75-GFP from the TGN. These observations and our previous experiments suggest that the normal role of Golgi LIMK1 is to slow-down cofilin-dependent actin turnover to maintain a population of actin filaments required for dynamin 2-mediated fission from the TGN.

DISCUSSION

Our results demonstrate an important new function of LIMK1 and its substrate cofilin in regulating protein trafficking at the Golgi apparatus. This trafficking role is highly selective for a subgroup of apical PM proteins that currently includes p75 and the related protein NHR2 (Figures 1 and 2) and is enhanced by the ability of LIMK1, not shared by LIMK2, to bind Golgi membranes (Figure 3, D and E). High-resolution live imaging experiments demonstrated that decreased LIMK1 activity or increased cofilin function dramatically disrupted the formation of tubular precursors to post-Golgi carriers for p75-GFP (Figure 4, A and B), the segregation of p75-GFP from TGN resident proteins (Figure 4, C and D), and the release of p75-GFP carriers into the cytoplasm (Figure 4E). A model summarizing our observations on the various molecules involved in p75 vesicular release from the TGN is represented in Figure 7.

Our experiments also suggest a subtle cooperation between LIMK, dynamin 2, and the dynamin-interacting proteins cortactin and syndapin 2 in p75-GFP carrier vesicle fission from the TGN. First, overexpression of wild-type dynamin 2 resulted in increased numbers of p75-GFP carrier vesicles released into the cytoplasm but this effect was suppressed by coexpression of LIMK1-KD (Figure 5A), in part by decreasing the recruitment of endogenous dynamin 2 to the Golgi (Figure 5C). Second, overexpression of a cortactin mutant that effectively binds actin filaments but cannot interact with dynamin 2 disrupted p75 carrier formation (Figure 5E), in agreement with recent observations by Cao *et al*. (2005), demonstrating a role of actin and cortactin in recruiting dynamin 2 to the Golgi. Third, we found that overexpression of syndapin 2's SH3 domain (which binds dynamin's PRD), or of dynamin's PRD, inhibited p75 vesicle

release from the TGN (Figure 5, E and B). One possibility to explain these effects is a disruption of syndapin 2/dynamin 2 complexes, which support dynamin's functions and provide functional coupling of dynamin to actin filament formation (Kessels *et al*., 2006). That the coupling between syndapin's SH3 domain and dynamin 2's PRD might be required for p75 post-Golgi carrier formation is also supported by our observation that overexpression of mutant dynamin 2 lacking just the PRD, i.e., with intact GTPase and oligomerization domains, also inhibited p75-GFP trafficking. Future experiments should test specifically whether syndapin 2's requirement for p75 exit from the TGN is solely explained by its participation in the recruitment of dynamin 2 or may also reflect its participation in the bending of TGN membranes via its BAR domain to form tubular carriers characteristic for p75 transport.

The key link between our trafficking observations with LIMK1/cofilin and with dynamin 2/syndapin 2/cortactin is actin. Experiments with actin toxins suggested that the trafficking effects of LIMK1-KD or cofilin S3A we observed were due to increased depolymerization of peri-Golgi actin filaments (Figure 6, A and B), in agreement with a recent report (Lazaro-Dieguez *et al*., 2007). This was rigorously confirmed by direct measurement of actin dynamics in the Golgi region using an MDCK cell line that expresses actin-paGFP (Figure 6, C and D). Actin-GFP is a good probe to study actin dynamics, as it has been used to study the role of actin dynamics in endocytosis and cell–cell adhesion (Yamada *et al*., 2005; Okreglak and Drubin, 2007). We found that the diffusion rate of Golgi actin-paGFP ($D \sim 1.7 \times 10^{-9}$ cm^2 s^{-1} in control cells) was significantly enhanced in the presence of either cofilin S3A ($D \sim 2.1 \times 10^{-9}$ cm^2 s^{-1}) or latrunculin B ($D \sim 2.6 \times 10^{-9}$ cm^2 s^{-1}): our control values are comparable with previously reported data obtained using fluorescence photobleaching recovery (Kreis *et al*., 1982). Together, our experiments strongly suggest that the normal role of Golgi LIMK1 is to maintain an ideal cofilin activity level to maintain a population of actin filaments (Percival *et al*., 2004) required for dynamin mediated, cortactin/syndapin 2-supported trafficking of selected PM cargo proteins out of the TGN.

Cdc42 is known to localize throughout the Golgi stack (Matas *et al*., 2004), whereas our experiments indicate that LIMK1 localizes to the TGN (Figure 3, D and E; data not shown). Furthermore, it has been shown that PAK4, a novel effector for cdc42, localizes to the Golgi complex (Abo *et al*., 1998), and stimulates LIMK1's ability to phosphorylate cofilin (Dan *et al*., 2001). Together, these observations raise the possibility that cdc42 and LIMK1 cooperate in post-Golgi transport at the TGN, similarly to the cooperation between cdc42 and N-WASP in Golgi–ER transport at the *cis*-Golgi (Luna *et al*., 2002).

Our results clearly advance the trafficking field in several novel areas beyond the previous study by Rosso *et al*. (2004). First, we conclusively showed that the trafficking role of LIMK1 takes place at the Golgi level, by excluding possible effects on protein synthesis or ER–Golgi transport, and by showing directly that inhibition of LIMK1 function decreases the kinetics of Golgi exit of PM markers. Second, we showed that the specific trafficking role of LIMK1-cofilin was on the fission of carrier vesicles from the TGN (Figure 4). Third, we demonstrated a possible cooperation between LIMK1 and dynamin 2 in this fission process (Figure 5). Fourth, we further characterized this fission mechanism by demonstrating that syndapin 2 and cortactin mutants mimic the effect of LIMK1-KD in the Golgi exit of p75-GFP. Fifth, we characterized the actin dynamics at the Golgi region using actin coupled to photoactivatable GFP. This approach allowed us to conclusively show that LIMK1-cofilin increase the dynamics of actin depolymerization at the Golgi, thus eliminating the alternative possibility suggested by Condeelis (Ghosh *et al*., 2004). Our observations suggest a mechanism to generate the population of actin filaments at the Golgi complex described by Stow and coworkers (Percival *et al*., 2004).

In summary, our experiments suggest a model (Figure 7) in which specialized organizations of actin filaments at the Golgi complex play very specific roles in promoting the trafficking of groups of PM proteins from the TGN to the PM. It is likely that other specialized actin organizations will play comparable roles in transport routes out of the other major sorting compartment of epithelial cells, common recycling endosomes (Cancino *et al*., 2007; Gravotta *et al*., 2007). An important objective for the future is to understand how the selectivity of a particular organization of the actin cytoskeleton for a particular cargo is established. In particular, we want to know how p75 sorting signals, previously defined as the *O*-glycan cluster in its ectodomin (Yeaman *et al*., 1997) upon clustering with galectin 3 (Delacour *et al*., 2007) are coupled to the actin regulatory mechanisms required for vesicle fission. Another major challenge is to identify the mechanisms that couple the actin-dependent fission mechanisms described here with our recent observation that kinesin 5B is essential for generation and transport of p75 carrier vesicles from Golgi to PM (Jaulin *et al*., 2007). In this regard, it is interesting to mention a recent report that postulates a role for LIMK1 in coordinating MT and actin cytoskeleton function (Gorovoy *et al*., 2005).

ACKNOWLEDGMENTS

We thank Dr. Diego Gravotta for invaluable help with the pulse-chase experiments, Dr. Ami Deora for help with the design of oligonucleotides used to knock down LIM kinases, Dr. Larry Leung for preparation of a cell line expressing galactosyl transferase, and Dr. Mark McNiven for generously providing cortactin antibodies and constructs. Our special thanks go to Isha Lucia Thorne for lending us her mother, Dr. Aparna Lakkaraju, to help with the artistic design of Figure 7. Dr. Rodriguez-Boulan was supported by Natioanl Institutes of Health grants GM-34107 and EY-08538, by the Research to Prevent Blindness Foundation, and by the Dyson Foundation. M.M.K. was supported by the Deutsche Forschungsgemeinschaft (DFG) and B. Q. was supported by the DFG and the Kultusministerium of the Land Sachsen-Anhalt.

REFERENCES

Abo, A., Qu, J., Cammarano, M. S., Dan, C., Fritsch, A., Baud, V., Belisle, B., and Minden, A. (1998). PAK4, a novel effector for Cdc42Hs, is implicated in the reorganization of the actin cytoskeleton and in the formation of filopodia. EMBO J. *17*, 6527–6540.

Acevedo, K., Moussi, N., Li, R., Soo, P., and Bernard, O. (2006). LIM kinase 2 is widely expressed in all tissues. J. Histochem. Cytochem. *54*, 487–501.

Allan, V. J., Thompson, H. M., and McNiven, M. A. (2002). Motoring around the Golgi. Nat. Cell Biol. *4*, E236–E242.

Arber, S., Barbayannis, F. A., Hanser, H., Schneider, C., Stanyon, C. A., Bernard, O., and Caroni, P. (1998). Regulation of actin dynamics through phosphorylation of cofilin by LIM-kinase. Nature *393*, 805–809.

Bamburg, J. R. (1999). Proteins of the ADF/cofilin family: essential regulators of actin dynamics. Annu. Rev. Cell Dev. Biol. *15*, 185–230.

Bernard, O. (2007). Lim kinases, regulators of actin dynamics. Int. J. Biochem. Cell Biol. *39*, 1071–1076.

Bonazzi, M. *et al*. (2005). CtBP3/BARS drives membrane fission in dynamin-independent transport pathways. Nat. Cell Biol. *7*, 570–580.

Bonifacino, J. S., and Traub, L. M. (2003). Signals for sorting of transmembrane proteins to endosomes and lysosomes. Annu. Rev. Biochem. *72*, 395–447.

Cancino, J., Torrealba, C., Soza, A., Yuseff, I., Gravotta, D., Henklein, P., Rodriguez-Boulan, E., and Gonzalez, A. (2007). Antibody to AP1B adaptor

blocks biosynthetic and recycling routes of basolateral proteins at recycling endosomes. Mol. Biol. Cell *18*, 4872–4884.

Cao, H., Thompson, H. M., Krueger, E. W., and McNiven, M. A. (2000). Disruption of Golgi structure and function in mammalian cells expressing a mutant dynamin. J. Cell Sci. *113*, 1993–2002.

Cao, H., Orth, J. D., Chen, J., Weller, S. G., Heuser, J. E., and McNiven, M. A. (2003). Cortactin is a component of clathrin-coated pits and participates in receptor-mediated endocytosis. Mol. Cell. Biol. *23*, 2162–2170.

Cao, H., Weller, S., Orth, J. D., Chen, J., Huang, B., Chen, J. L., Stamnes, M., and McNiven, M. A. (2005). Actin and Arf1-dependent recruitment of a cortactin-dynamin complex to the Golgi regulates post-Golgi transport. Nat. Cell Biol. *7*, 483–492.

Carlier, M. F., Laurent, V., Santolini, J., Melki, R., Didry, D., Xia, G. X., Hong, Y., Chua, N. H., and Pantaloni, D. (1997). Actin depolymerizing factor (ADF/cofilin) enhances the rate of filament turnover: implication in actin-based motility. J. Cell Biol. *136*, 1307–1322.

Carreno, S., Engqvist-Goldstein, A. E., Zhang, C. X., McDonald, K. L., and Drubin, D. G. (2004). Actin dynamics coupled to clathrin-coated vesicle formation at the trans-Golgi network. J. Cell Biol. *165*, 781–788.

Chen, X., and Macara, I. G. (2006). Par-3 mediates the inhibition of LIM kinase 2 to regulate cofilin phosphorylation and tight junction assembly. J. Cell Biol. *172*, 671–678.

Conner, S. D., and Schmid, S. L. (2003). Regulated portals of entry into the cell. Nature *422*, 37–44.

Dan, C., Kelly, A., Bernard, O., and Minden, A. (2001). Cytoskeletal changes regulated by the PAK4 serine/threonine kinase are mediated by LIM kinase 1 and cofilin. J. Biol. Chem. *276*, 32115–32121.

Deborde, S., Perret, E., Gravotta, D., Deora, A., Salvarezza, S., Schreiner, R., and Rodriguez-Boulan, E. (2008). Clathrin is a key regulator of basolateral polarity. Nature *452*, 719–723.

Delacour, D., Cramm-Behrens, C. I., Drobecq, H., Le Bivic, A., Naim, H. Y., and Jacob, R. (2006). Requirement for galectin-3 in apical protein sorting. Curr. Biol. *16*, 408–414.

Delacour, D. *et al*. (2005). Galectin-4 and sulfatides in apical membrane trafficking in enterocyte-like cells. J. Cell Biol. *169*, 491–501.

Delacour, D., Greb, C., Koch, A., Salomonsson, E., Leffler, H., Le Bivic, A., and Jacob, R. (2007). Apical sorting by galectin-3-dependent glycoprotein clustering. Traffic *8*, 379–388.

Egea, G., Lazaro-Dieguez, F., and Vilella, M. (2006). Actin dynamics at the Golgi complex in mammalian cells. Curr. Opin. Cell Biol. *18*, 168–178.

Erickson, J. W., Zhang, C., Kahn, R. A., Evans, T., and Cerione, R. A. (1996). Mammalian Cdc42 is a brefeldin A-sensitive component of the Golgi apparatus. J. Biol. Chem. *271*, 26850–26854.

Foletta, V. C., Moussi, N., Sarmiere, P. D., Bamburg, J. R., and Bernard, O. (2004). LIM kinase 1, a key regulator of actin dynamics, is widely expressed in embryonic and adult tissues. Exp. Cell Res. *294*, 392–405.

Ghosh, M., Song, X., Mouneimne, G., Sidani, M., Lawrence, D. S., and Condeelis, J. S. (2004). Cofilin promotes actin polymerization and defines the direction of cell motility. Science *304*, 743–746.

Gorovoy, M., Niu, J., Bernard, O., Profirovic, J., Minshall, R., Neamu, R., and Voyno-Yasenetskaya, T. (2005). LIM kinase 1 coordinates microtubule stability and actin polymerization in human endothelial cells. J. Biol. Chem. *280*, 26533–26542.

Gravotta, D., Deora, A., Perret, E., Oyanadel, C., Soza, A., Schreiner, R., Gonzalez, A., and Rodriguez-Boulan, E. (2007). AP1B sorts basolateral proteins in recycling and biosynthetic routes of MDCK cells. Proc. Natl. Acad Sci. USA *104*, 1564–1569.

Guerriero, C. J., Weixel, K. M., Bruns, J. R., and Weisz, O. A. (2006). Phosphatidylinositol 5-kinase stimulates apical biosynthetic delivery via an Arp2/3-dependent mechanism. J. Biol. Chem. *281*, 15376–15384.

Itoh, T., Erdmann, K. S., Roux, A., Habermann, B., Werner, H., and De Camilli, P. (2005). Dynamin and the actin cytoskeleton cooperatively regulate plasma membrane invagination by BAR and F-BAR proteins. Dev. Cell *9*, 791–804.

Jaulin, F., Xue, X., Rodriguez-Boulan, E., and Kreitzer, G. (2007). Polarization-dependent selective transport to the apical membrane by KIF5B in MDCK Cells. Dev. Cell *13*, 511–522.

Kaksonen, M., Toret, C. P., and Drubin, D. G. (2005). A modular design for the clathrin- and actin-mediated endocytosis machinery. Cell *123*, 305–320.

Kessels, M. M., Dong, J., Leibig, W., Westermann, P., and Qualmann, B. (2006). Complexes of syndapin II with dynamin II promote vesicle formation at the trans-Golgi network. J. Cell Sci. *119*, 1504–1516.

Kreis, T. E., Geiger, B., and Schlessinger, J. (1982). Mobility of microinjected rhodamine actin within living chicken gizzard cells determined by fluorescence photobleaching recovery. Cell *29*, 835–845.

Kreitzer, G., Marmorstein, A., Okamoto, P., Vallee, R., and Rodriguez-Boulan, E. (2000). Kinesin and dynamin are required for post-Golgi transport of a plasma-membrane protein. Nat. Cell Biol. *2*, 125–127.

Kreitzer, G., Schmoranzer, J., Low, S. H., Li, X., Gan, Y., Weimbs, T., Simon, S. M., and Rodriguez-Boulan, E. (2003). Three-dimensional analysis of post-Golgi carrier exocytosis in epithelial cells. Nat. Cell Biol. *5*, 126–136.

Kroschewski, R., Hall, A., and Mellman, I. (1999). Cdc42 controls secretory and endocytic transport to the basolateral plasma membrane of MDCK cells. Nat. Cell Biol. *1*, 8–13.

Lappalainen, P., and Drubin, D. G. (1997). Cofilin promotes rapid actin filament turnover in vivo. Nature *388*, 78–82.

Lazaro-Dieguez, F., Colonna, C., Cortegano, M., Calvo, M., Martinez, S. E., and Egea, G. (2007). Variable actin dynamics requirement for the exit of different cargo from the trans-Golgi network. FEBS Lett. *581*, 3875–3881.

Luna, A., Matas, O. B., Martinez-Menarguez, J. A., Mato, E., Duran, J. M., Ballesta, J., Way, M., and Egea, G. (2002). Regulation of protein transport from the Golgi complex to the endoplasmic reticulum by CDC42 and N-WASP. Mol. Biol. Cell *13*, 866–879.

Matas, O. B., Martinez-Menarguez, J. A., and Egea, G. (2004). Association of Cdc42/N-WASP/Arp2/3 signaling pathway with Golgi membranes. Traffic *5*, 838–846.

McGrath, J. L., Hartwig, J. H., Tardy, Y., and Dewey, C. F., Jr. (1998). Measuring actin dynamics in endothelial cells. Microsc. Res. Tech. *43*, 385–394.

McNiven, M. A., and Thompson, H. M. (2006). Vesicle formation at the plasma membrane and trans-Golgi network: the same but different. Science *313*, 1591–1594.

Merrifield, C. J., Perrais, D., and Zenisek, D. (2005). Coupling between clathrin-coated-pit invagination, cortactin recruitment, and membrane scission observed in live cells. Cell *121*, 593–606.

Murray, S. S., Perez, P., Lee, R., Hempstead, B. L., and Chao, M. V. (2004). A novel p75 neurotrophin receptor-related protein, NRH2, regulates nerve growth factor binding to the TrkA receptor. J. Neurosci. *24*, 2742–2749.

Musch, A. (2004). Microtubule organization and function in epithelial cells. Traffic *5*, 1–9.

Musch, A., Cohen, D., Kreitzer, G., and Rodriguez-Boulan, E. (2001). cdc42 regulates the exit of apical and basolateral proteins from the trans-Golgi network. EMBO J. *20*, 2171–2179.

Noda, Y., Okada, Y., Saito, N., Setou, M., Xu, Y., Zhang, Z., and Hirokawa, N. (2001). KIFC3, a microtubule minus end-directed motor for the apical transport of annexin XIIIb-associated Triton-insoluble membranes. J. Cell Biol. *155*, 77–88.

Okreglak, V., and Drubin, D. G. (2007). Cofilin recruitment and function during actin-mediated endocytosis dictated by actin nucleotide state. J. Cell Biol. *178*, 1251–1264.

Patterson, G. H., and Lippincott-Schwartz, J. (2002). A photoactivatable GFP for selective photolabeling of proteins and cells. Science *297*, 1873–1877.

Percival, J. M., Hughes, J. A., Brown, D. L., Schevzov, G., Heimann, K., Vrhovski, B., Bryce, N., Stow, J. L., and Gunning, P. W. (2004). Targeting of a tropomyosin isoform to short microfilaments associated with the Golgi complex. Mol. Biol. Cell *15*, 268–280.

Perret, E., Lakkaraju, A., Deborde, S., Schreiner, R., and Rodriguez-Boulan, E. (2005). Evolving endosomes: how many varieties and why? Curr. Opin. Cell Biol. *17*, 423–434.

Qualmann, B., and Kelly, R. B. (2000). Syndapin isoforms participate in receptor-mediated endocytosis and actin organization. J. Cell Biol. *148*, 1047–1062.

Qualmann, B., Kessels, M. M., and Kelly, R. B. (2000). Molecular links between endocytosis and the actin cytoskeleton. J. Cell Biol. *150*, F111–116.

Rodriguez-Boulan, E., Kreitzer, G., and Musch, A. (2005). Organization of vesicular trafficking in epithelia. Nat. Rev. Mol. Cell Biol. *6*, 233–247.

Rosso, S., Bollati, F., Bisbal, M., Peretti, D., Sumi, T., Nakamura, T., Quiroga, S., Ferreira, A., and Caceres, A. (2004). LIMK1 regulates Golgi dynamics, traffic of Golgi-derived vesicles, and process extension in primary cultured neurons. Mol. Biol. Cell *15*, 3433–3449.

Rozelle, A. L., Machesky, L. M., Yamamoto, M., Driessens, M. H., Insall, R. H., Roth, M. G., Luby-Phelps, K., Marriott, G., Hall, A., and Yin, H. L. (2000). Phosphatidylinositol 4,5-bisphosphate induces actin-based movement of raft-enriched vesicles through WASP-Arp2/3. Curr. Biol. *10*, 311–320.

Scheiffele, P., Peranen, J., and Simons, K. (1995). N-glycans as apical sorting signals in epithelial cells. Nature *378*, 96–98.

Simons, K., and Ikonen, E. (1997). Functional rafts in cell membranes. Nature *387*, 569–572.

Song, B. D., Leonard, M., and Schmid, S. L. (2004). Dynamin GTPase domain mutants that differentially affect GTP binding, GTP hydrolysis, and clathrin-mediated endocytosis. J. Biol. Chem. *279*, 40431–40436.

Spector, I., Braet, F., Shochet, N. R., and Bubb, M. R. (1999). New anti-actin drugs in the study of the organization and function of the actin cytoskeleton. Microsc. Res. Tech. *47*, 18–37.

Stamnes, M. (2002). Regulating the actin cytoskeleton during vesicular transport. Curr. Opin. Cell Biol. *14*, 428–433.

Sumi, T., Matsumoto, K., Takai, Y., and Nakamura, T. (1999). Cofilin phosphorylation and actin cytoskeletal dynamics regulated by rho- and Cdc42-activated LIM-kinase 2. J. Cell Biol. *147*, 1519–1532.

Tai, A. W., Chuang, J. Z., and Sung, C. H. (2001). Cytoplasmic dynein regulation by subunit heterogeneity and its role in apical transport. J. Cell Biol. *153*, 1499–1509.

Tomiyoshi, G., Horita, Y., Nishita, M., Ohashi, K., and Mizuno, K. (2004). Caspase-mediated cleavage and activation of LIM-kinase 1 and its role in apoptotic membrane blebbing. Genes Cells *9*, 591–600.

Ya-Wen Liu, M.C.S., Schroeter, T., Lukiyanchuk, V., and Sandra Schmid, L. (2008). Isoform and splice-variant specific functions of dynamin-2 revealed by analysis of conditional knock-out cells. Mol. Biol. Cell *19*, 5347–5359.

Yamada, S., Pokutta, S., Drees, F., Weis, W. I., and Nelson, W. J. (2005). Deconstructing the cadherin-catenin-actin complex. Cell *123*, 889–901.

Yang, J. S., Zhang, L., Lee, S. Y., Gad, H., Luini, A., and Hsu, V. W. (2006). Key components of the fission machinery are interchangeable. Nat. Cell Biol. *8*, 1376–1382.

Yarar, D., Waterman-Storer, C. M., and Schmid, S. L. (2005). A dynamic actin cytoskeleton functions at multiple stages of clathrin-mediated endocytosis. Mol. Biol. Cell *16*, 964–975.

Yeaman, C., Le Gall, A. H., Baldwin, A. N., Monlauzeur, L., Le Bivic, A., and Rodriguez-Boulan, E. (1997). The O-glycosylated stalk domain is required for apical sorting of neurotrophin receptors in polarized MDCK cells. J. Cell Biol. *139*, 929–940.